

## Oxidatively-Promoted CO-Substitution Reaction by PPh<sub>3</sub> in the Dinuclear FvCo<sub>2</sub>(CO)<sub>4</sub> in Low-Polarity Media Comprising CH<sub>2</sub>Cl<sub>2</sub>/[NBu<sub>4</sub>][B(C<sub>6</sub>F<sub>5</sub>)<sub>4</sub>]<sup>†</sup>

Sameerah I. Al-Saeed<sup>1</sup>, Ali M. Alsalmeh<sup>2</sup> and Ayman Nafady<sup>2,3\*</sup>

<sup>1</sup>Department of Chemistry, College of Science, Princess Nora bint Abdulrahman University, Riyadh, Saudi Arabia

<sup>2</sup>Department of Chemistry, College of Science, King Saud University, Riyadh, Saudi Arabia

<sup>3</sup>Department of Chemistry, Faculty of Science, Sohag University, Cairo, Egypt

\*E-mail: [anafady@ksu.edu.sa](mailto:anafady@ksu.edu.sa)

Received: 10 November 2014 / Accepted: 29 November 2014 / Published: 30 December 2014

Electrochemically-promoted CO-substitution of FvCo<sub>2</sub>(CO)<sub>4</sub>, **1**, by using PPh<sub>3</sub> in media composing of CH<sub>2</sub>Cl<sub>2</sub> and the weakly coordinating [NBu<sub>4</sub>][B(C<sub>6</sub>F<sub>5</sub>)<sub>4</sub>] electrolyte has been achieved on both cyclic voltammetry (CV) and bulk electrolysis time scales. Using CV and in the presence of 1 equiv of PPh<sub>3</sub>, the substitution reaction is very simple, leading to the stable mono-substituted product, [FvCo<sub>2</sub>(CO)<sub>3</sub>PPh<sub>3</sub>]<sup>+</sup>, **2**<sup>+</sup>, which can be either reversibly oxidized ( $E_{1/2} = 0.2$  V) to the mono-substituted dication, [FvCo<sub>2</sub>(CO)<sub>3</sub>PPh<sub>3</sub>]<sup>2+</sup>, **2**<sup>2+</sup>, or reduced to the neutral FvCo<sub>2</sub>(CO)<sub>3</sub>PPh<sub>3</sub>, **2** at  $E_{1/2} = -0.35$  V vs Fc<sup>0/+</sup>. Generation of these substitution products in the bulk electrolysis time scale allowed for facile measurements of their spectroscopic properties via IR and ESR spectroscopy. IR data revealed that the final product of the oxidative bulk electrolysis is the monosubstituted dication, **2**<sup>2+</sup>, with IR bands at 2114, 2091 and 2063 cm<sup>-1</sup>. One-electron back-reduction of **2**<sup>2+</sup> to **2**<sup>+</sup> allowed for spectral identification of the radical monocation via IR and ESR. The fluid and frozen ESR spectra of **2**<sup>+</sup> are in a good agreement with its IR data and consistent with having a *transoid* configuration. Finally, the neutral monosubstituted, **2**, gave IR bands confirming the presence of one Co(CO)(PPh<sub>3</sub>) moiety at 1925cm<sup>-1</sup> and one Co(CO)<sub>2</sub> group at 2022 and 1958 cm<sup>-1</sup>, respectively. Importantly, this work clearly demonstrates that "electrochemical switch" approach can be applied to undertake and probe CO-substitution by the stronger PPh<sub>3</sub> nucleophile for the dinuclear FvCo<sub>2</sub>(CO)<sub>4</sub> system. This significant outcome is made possible by the greatly enhanced stability of the generated radical cations of **1** in media comprising gentle solvent and supporting electrolyte.

### Keywords:

Oxidatively-induced, CO-substitution reaction, bimetallic, FvCo<sub>2</sub>(CO)<sub>4</sub>, weakly coordinating anions

<sup>†</sup>Dedicated to Prof. William E. Geiger, University of Vermont, USA in recognition of his outstanding contribution to the field of organometallic electrochemistry.

## 1. INTRODUCTION

Over the past few decades, photochemical and thermal activations have been widely utilized to undertake substitution reactions of inorganic and organometallic complexes [1-3]. In such reactions, the substitution usually occurs by dissociative or associative pathways involving loss of a ligand from the excited state or ligand addition to excited state as the key step [4, 5]. In this context, thermally driven substitution of one or more CO groups by phosphine ligands in the mononuclear  $\text{CpCo}(\text{CO})_2$  is known to be slow (e.g., 24 h reflux) and leads to formation of a mixture of products including the mono- and di-substituted products [6].

Recently, substitution processes induced by electron-transfer have rapidly become an important reaction in organometallic substitution chemistry. Electrochemical tools such as cyclic voltammetry (CV), double potential step chronocoulometry (DPSCA), and bulk electrolysis (BE) have been successfully employed not only to induce and monitor the progress of these ligand exchange reactions, but also to measure the kinetics of the electron transfer [7-10]. From these studies, it is generally understood that oxidatively-induced substitutions proceed via an odd-electron radical intermediates and that the mechanism, in most cases, is associative [11].

Although ligand substitutions of mononuclear complexes have been extensively studied [7-11], very little quantitative information is available concerning ligand substitutions of the dinuclear analogues. In this respect, Vahrenkamp and co-workers [12, 13] have studied the substitution of the dinuclear complex  $\text{FeCo}(\text{CO})_7(\mu\text{-AsMe}_2)$  by  $\text{PMe}_3$  and  $\text{P}(\text{OMe})_3$ . They demonstrated that the CO ligand substitutions occur through three stepwise sequences of metal-metal bond breaking and subsequent bond re-forming with loss of CO. Also Baker and his co-workers [14] have found out that the  $33 e^-$  dinuclear radical  $\text{Fe}_2(\text{CO})_7(\mu\text{-PPh}_2)$  undergoes rapid CO ligand substitution with a variety of tertiary phosphorous ligands to give mono- and di-substituted  $33 e^-$  products. It was then demonstrated that electron-transfer-catalyzed nucleophilic substitution in bi- and poly-nuclear metal carbonyls is a rather general reaction and can lead to very promising results [15].

Our previous work on the electrochemical oxidation of  $\text{FvCo}_2(\text{CO})_4$ , **1**, in media comprising  $\text{CH}_2\text{Cl}_2/[\text{NBu}_4][\text{B}(\text{C}_6\text{F}_5)_4]$  has showed that both the one-electron,  $\mathbf{1}^+$  and two-electron,  $\mathbf{1}^{2+}$  oxidation products are persistent in solution and adopting the *cisoid* structure to allow for full Co-Co bond formation in the dication  $\mathbf{1}^{2+}$  [16]. Given the well-known increase in the liability of carbonyls in 17-electron radicals, as seen in the parent  $\text{CpCo}(\text{CO})_2$  case [17-20], it seemed reasonable to investigate the possibility of oxidatively-induced CO-substitution reactions by strong nucleophiles such as  $\text{PPh}_3$  in the oxidation products of  $\text{FvCo}_2(\text{CO})_4$ , **1**. Indeed, this dinuclear complex,  $\text{FvCo}_2(\text{CO})_4$ , **1** is an attractive candidate for the mechanistic study of CO-substitution reactions due to the hypothesis that, in principle, one might be able to measure the substitution rates of both the monocation  $\mathbf{1}^+$  and the dication  $\mathbf{1}^{2+}$ . Furthermore, the anticipated high stability of these substitution products, particularly in the presence of weakly coordinating  $[\text{B}(\text{C}_6\text{F}_5)_4]^-$  anion, is likely to provide an opportunity for detailed characterization of their molecular structures by several spectroscopic techniques such as IR, ESR and NMR spectroscopy.

## 2. EXPERIMENTAL

This work was undertaken at Prof. W. E. Geiger's laboratory at the University of Vermont, USA.

A full description of the experimental procedures used in this work is available in a previous paper [16]. The other details are as follows.

All experiments were conducted under nitrogen using either standard Schlenk techniques or a Vacuum Atmospheres drybox. Reagent-grade dichloromethane ( $\text{CH}_2\text{Cl}_2$ ) is dried over  $\text{CaH}_2$  and then vacuum distilled.  $\text{FvCo}_2(\text{CO})_4$ , **1**, had been prepared based on literature procedure [16]. It was purified by vacuum sublimation and checked for purity by NMR, IR, and C, H analysis.  $[\text{NBu}_4][\text{B}(\text{C}_6\text{F}_5)_4]$  was prepared by metathesis of  $[\text{NBu}_4]\text{Br}$  with  $\text{K}[\text{B}(\text{C}_6\text{F}_5)_4]$  (Boulder Scientific, Boulder, Co) and purified as detailed elsewhere [21]. Electrochemical measurements were conducted inside a drybox using a standard three-electrode cell configuration and a PARC 273A potentiostat interfaced to a personal computer. The glassy carbon working electrodes (1.5 mm diameter, Cypress, or 1 mm diameter, from Bioanalytical Systems) are routinely polished with Buehler diamond paste, followed by washings with nanopure water, and dried under vacuum. The working electrode for bulk electrolysis was a Pt-basket.

All potentials given in this paper are referenced versus ferrocene/ferrocenium( $\text{Fc}^{0/+}$ ) couple. Mechanistic aspects associated with the redox processes were obtained via cyclic voltammetry (CV) and linear sweep voltammetric (LSV) data. Diagnostic criteria such as shapes and scan rate responses of the CV curves were accomplished via protocols described in reference [22]. IR spectra were recorded with an ATI-Mattson Infinity Series FTIR interfaced to a computer, using Winfirst software at a resolution of  $4\text{ cm}^{-1}$ .

## 3. RESULTS AND DISCUSSION

### 3.1. Electrochemical CO-Substitution by $\text{PPh}_3$ .

The electrochemically-induced CO-substitution by  $\text{PPh}_3$  can be observed directly by carrying out cyclic voltammetry of the bimetallic complex,  $\text{FvCo}_2(\text{CO})_4$ , **1**, in the presence of added  $\text{PPh}_3$  in  $\text{CH}_2\text{Cl}_2$  containing the  $[\text{NBu}_4][\text{B}(\text{C}_6\text{F}_5)_4]$  electrolyte at ambient temperature using different scan rates (0.1-1 V/s).

#### 3.1.1. Cyclic Voltammetry

Figure 1 illustrates how the presence of 1 equiv of  $\text{PPh}_3$  leads to alteration of the reversible CV waves of **1**. In particular, the first oxidation wave, **A**, loses its chemical reversibility as indicated by the virtual absence of the cathodic counterpart, wave  $\text{A}_{\text{red}}$ . The second oxidation wave of **1** (wave **B**) is still reversible but its intensity diminished in proportion to the concentration of  $\text{PPh}_3$ . The resulting substitution product, **2**, has two new reversible CV waves. The first wave, **C**, is detected during the anodic forward scan of **1** at potential ( $E_{1/2} = 0.20\text{ V}$ ) that is more positive than wave **A** ( $E_{1/2} = 0.061\text{ V}$ )

while the second wave, **D**, was observed on the reverse scan at a potential that is more negative ( $E_{1/2} = -0.35$  V) than the first oxidation wave of **1** (wave **A**) as illustrated in Figure 1(b).

The formation of the substitution product, **2**, can be easily monitored by gradual addition of  $\text{PPh}_3$  (0.25 to 1 equiv) as shown in Fig. 2(a). The current of the waves **C** and **D** of the substitution product markedly increased as the concentration of the added  $\text{PPh}_3$  increased from 0.25 to 1.0 equiv, thereby indicating that addition of 0.25 to 1 equiv of  $\text{PPh}_3$  produces only one product in the CV time scale, which is expected to be the mono-substituted complex  $[\text{FvCo}_2(\text{CO})_3(\text{PPh}_3)]^{2+}$ , **2**<sup>+</sup>. On this basis, we assign wave **C** ( $E_{1/2} = 0.20$  V) to the oxidation of the  $\text{PPh}_3$ -substituted monocation to dication i.e., **2**<sup>+</sup>/**2**<sup>2+</sup> and wave **D** ( $E_{1/2} = -0.35$  V) to the reduction of **2**<sup>+</sup> to the neutral mono-substitution product  $\text{FvCo}_2(\text{CO})_3(\text{PPh}_3)$ , **2**.

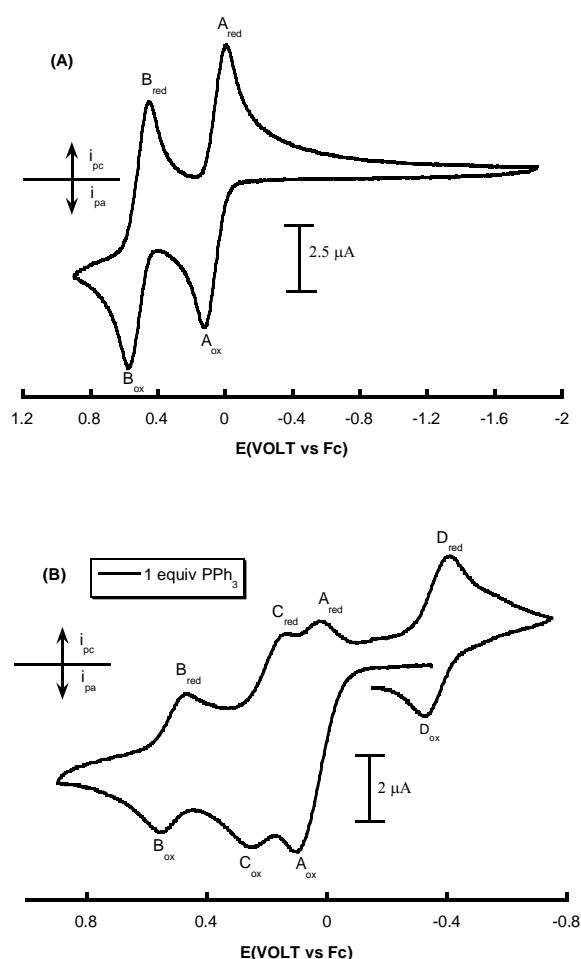


**Figure 1.** (a) Cyclic voltammogram of 1 mM **1** in  $\text{CH}_2\text{Cl}_2/0.05$  M  $[\text{NBu}_4][\text{B}(\text{C}_6\text{F}_5)_4]$  at scan rate of 500 mV/s on a 1 mm GC disk electrode before addition of  $\text{PPh}_3$ . (b) CV of **1** under the same condition and in presence of 1 equiv  $\text{PPh}_3$

Since the formation of the substitution product,  $2^+$ , is independent of the switching potentials, i.e. scanning through  $1/1^+$  and/or  $1^{2+}$  gives the same substitution products (Figure 2(b)) and the fact that the generation of  $1^+$  is occurring at potential ( $E_{1/2} = 0.06$  V) less than the most positive wave of the substitution product, wave C, ( $E_{1/2} = 0.20$  V), it follows that  $1^+$  is the species responsible for the ligand replacement reaction to afford the substitution products of **1**. Indeed, this was evidenced by the finding that the chemical reversibility of the wave attributed to the  $1^+/1^{2+}$  couple did not diminish with increasing the concentration of the added  $PPh_3$  up to 1 equiv. This means that the chance of the dication,  $1^{2+}$ , to react with the added  $PPh_3$  is minimal compared to  $1^+$  when the concentration of  $PPh_3$  is less than 1 equiv.

On the basis of a direct comparison of the cyclic voltammograms of **1** in the presence and the absence of 1 equiv of  $PPh_3$ , we found that ca. 30 % of the substitution product  $2^+$  is generated from the reaction of  $1^+$  and  $PPh_3$  on the CV time scale of seconds, thereby indicating that the substitution reaction by using  $PPh_3$  is very fast at room temperature and mostly likely is induced by the generation of the monocation  $1^+$ .

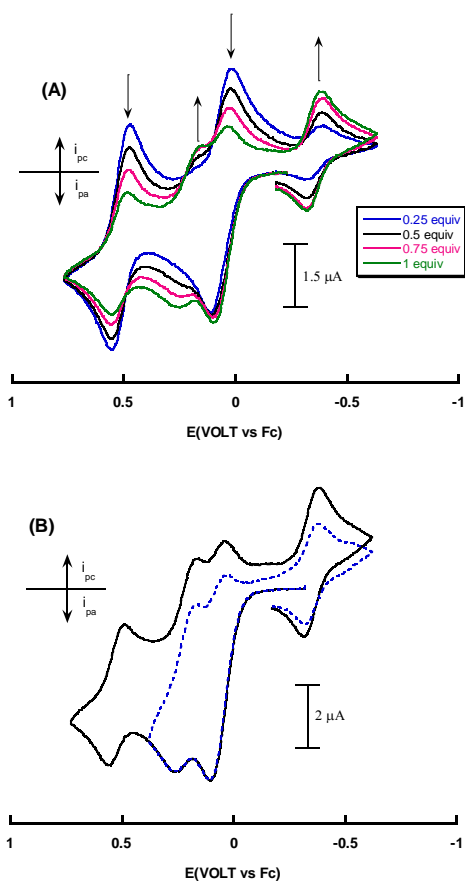


**Figure 2.** (a) Cyclic voltammograms of 0.55 mM **1** in  $CH_2Cl_2/0.05$  M  $[NBu_4][B(C_6F_5)_4]$  at scan rate of 500 mV/s, in presence of 0.25, 0.5, 0.75, 1 equiv  $PPh_3$  on a 1 mm GC disk (b) CV of 1.1 mM **1** in  $CH_2Cl_2/0.05$  M  $[NBu_4][B(C_6F_5)_4]$  at scan rate of 500 mV/s, 1 mm GC disk in presence of 1 equiv  $PPh_3$  at different switching potentials.

## 3.1.2. Bulk Electrolysis

Bulk electrolysis was conducted to investigate the long-term stability of the substitution product(s) and to probe their spectroscopic properties. The electrolysis of  $\text{FvCO}_2(\text{CO})_4$ , **1**, was undertaken at a potential that is more positive than the first oxidative wave in the presence of 1 equiv of  $\text{PPh}_3$  at either 298 or 273K. In the absence of  $\text{PPh}_3$  the oxidation of **1** to  $\mathbf{1}^+$  required 1 F mol<sup>-1</sup> ( $n=1$ ). In the presence of 1 equiv  $\text{PPh}_3$ , the exhaustive oxidation at  $E_{\text{app}} = +0.4$  V vs.  $\text{Fc}^{0/+}$  was completed after consumption of approximately 1.8 F mol<sup>-1</sup> of **1**. The color of the solution changed from orange to brown-olive. Cyclic and linear sweep voltammograms recorded after bulk-electrolysis (Figure 3) indicate the formation of a dication ( $\mathbf{1}^{2+}$ ) with two reversible reduction waves having formal potentials identical to those measured on the CV time scale, i.e.,  $E_{1/2}(1) = 0.20$  V,  $E_{1/2}(2) = -0.35$  V vs  $\text{Fc}^{0/+}$  respectively. Formation of the dication  $\mathbf{2}^{2+}$  after bulk electrolysis accounts for the increased coulomb count observed during the bulk electrolysis, since at  $E_{\text{app}} = 0.4$  V vs  $\text{Fc}^{0/+}$  the monocation  $\mathbf{2}^+$  is converted into  $\mathbf{2}^{2+}$  upon reaction with  $\text{PPh}_3$ .

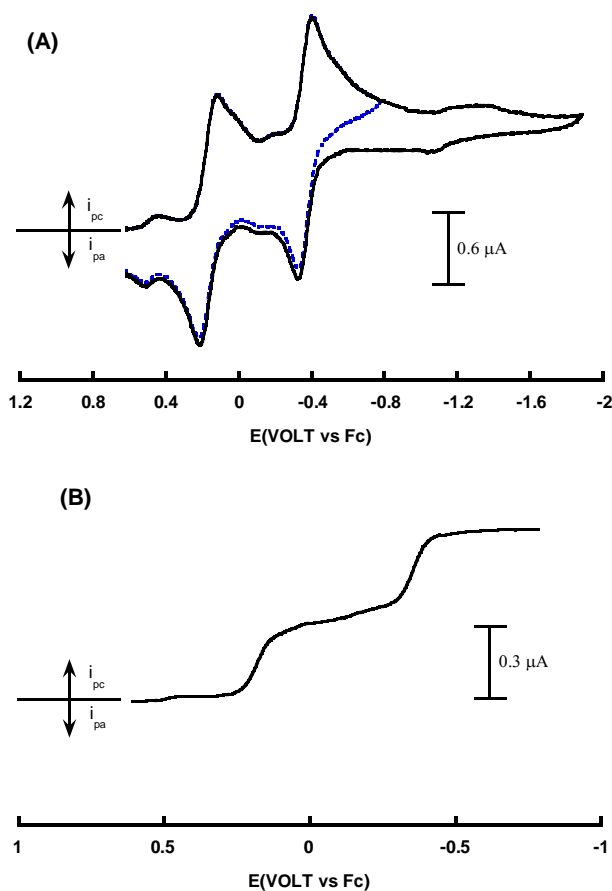


**Figure 3.** (a) Cyclic voltammograms of  $\mathbf{2}^{2+}$  recorded after bulk electrolysis of 1 mM **1** in  $\text{CH}_2\text{Cl}_2/0.05$  M  $[\text{NBu}_4][\text{B}(\text{C}_6\text{F}_5)_4]$  and 1 equiv  $\text{PPh}_3$  at scan rate of 100 mV/s, 1 mm GC disk electrode. (b) LSV under the same conditions at scan rate of 2 mV/s.

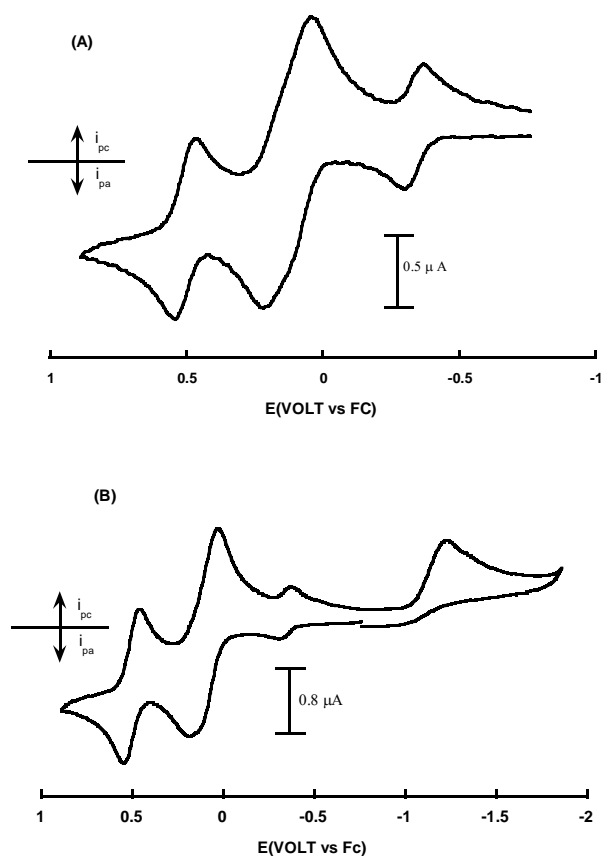


**Figure 4.** Cyclic voltammograms of the products generated after back reduction of  $2^{2+}$  at  $E_{app} = -0.7$  V vs  $Fc^{0/+}$  in  $CH_2Cl_2/0.05$  M  $[NBu_4][B(C_6F_5)_4]$  at scan rate of 100 mV/s on a 1 mm GC disk electrode.

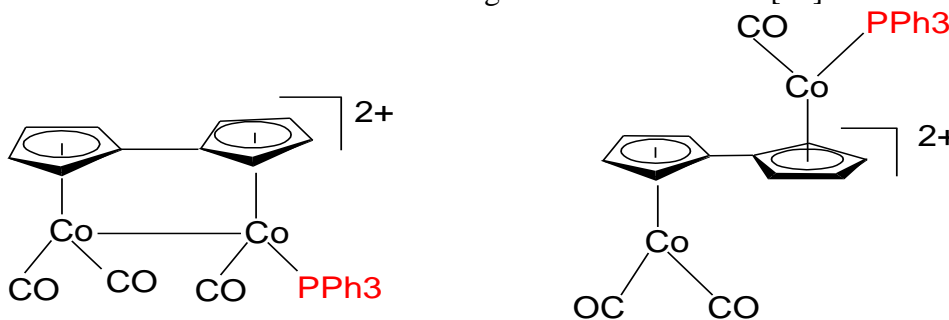
The first reduction wave ( $E_{1/2} = 0.20$  V) of the generated substitution product is assigned to the  $2^{2+}/2^+$  couple whereas the second wave ( $E_{1/2} = -0.35$  V) is attributed to the reduction of the monocation to the neutral species, i.e.,  $2^+/2$ . Based on comparisons of measured peak and plateau currents of the CV and LSV scans the yield of the substitution product was estimated to be  $\approx 35\%$ .

Back reduction of this  $PPh_3$ -substituted dication,  $2^{2+}$ , at potential of  $E_{app} = -0.7$  V vs.  $Fc^{0/+}$  (more negative than the second reduction wave of  $2^{2+}$ ) gives the neutral substituted product **2** (20%) and regenerates the original starting material, **1** (30%) in addition to an unidentified product that is detected at -1.2 V as an irreversible wave as shown in Figure 4.

### 3.2. Characterization of the substitution products

According to cyclic voltammetry and bulk electrolyses data, it is obvious that the electrochemical oxidation of **1** in the presence of 1 equiv of  $PPh_3$  leads to the formation of the mono-substitution product **2** that has two chemically and electrochemical reversible waves. The dication of

this substitution product,  $\mathbf{2}^{2+}$ , is very likely to have one of the two structures shown below, depending on whether or not substitution has resulted in cleavage of the Co-Co bond [16].



S1

S2

Since structure S2 essentially consists of two sections, one analogous to  $[\text{CpCo}(\text{CO})_2]^+$  [17, 18] and the other one analogous to  $[\text{CpCo}(\text{CO})(\text{PPh}_3)]^+$  [19, 20], we chose to compare the voltammetric and spectroscopic data of  $\mathbf{2}^{2+}$  with those of the mononuclear analogues. The fact that the cis-conformation, structure S1, has a metal-metal bond, it is expected that the voltammetric and spectral behavior of  $\mathbf{2}^{2+}$  to be different from the corresponding monocationic analogues, i.e.,  $[\text{CpCo}(\text{CO})_2]^+$  and  $[\text{CpCo}(\text{CO})(\text{PPh}_3)]^+$ .

The potential of the more negative process (wave **D**) of the dication  $\mathbf{2}^{2+}$  ( $E_{1/2} = -0.35$  V) is found to be identical with that measured for the oxidation of an authentic sample of  $\text{CpCo}(\text{CO})(\text{PPh}_3)$  under the same conditions, consistent with the wave arising from reduction of the  $[(\text{C}_5\text{H}_4)\text{Co}(\text{CO})(\text{PPh}_3)]^+$  side in structure S2. The potential of the more positive process (wave **C**) of  $\mathbf{2}^{2+}$  ( $E_{1/2} = 0.20$  V) is very close to that estimated for the oxidation of  $\text{CpCo}(\text{CO})_2$ , thereby indicating that this wave represents the reduction of the unsubstituted part of  $\mathbf{2}^{2+}$ , i.e.  $[(\text{C}_5\text{H}_4)\text{Co}(\text{CO})_2]^+$  in S2. Thus, the  $E_{1/2}$  values of the redox processes  $\mathbf{2}^{2+/+}$  and  $\mathbf{2}^{+/0}$  strongly support structure S2 for the product dication. This conclusion is further supported by IR spectra obtained during the bulk electrolysis. In this respect, the IR spectrum of **1** recorded before bulk electrolysis in the presence of 1 equiv of  $\text{PPh}_3$  shows only two carbonyl bands ( $2020, 1962\text{ cm}^{-1}$ ). This indicates that there is no reaction between the neutral starting material, **1**, and the added  $\text{PPh}_3$  (Fig. 5(a)). IR spectra obtained after bulk electrolysis at applied potential more positive than the  $E_{1/2}$  of  $\mathbf{1}^{2+}$  show the existence of three new IR bands ( $2114, 2091$  and  $2063\text{ cm}^{-1}$ ) that do not belong to either  $\mathbf{1}^+$  or  $\mathbf{1}^{2+}$  as illustrated in Figure 5(b). The two higher energy bands ( $2114, 2091\text{ cm}^{-1}$ ) are assigned to the  $[(\text{C}_5\text{H}_4)\text{Co}(\text{CO})_2]^+$  side of  $\mathbf{2}^{2+}$  and the  $2063\text{ cm}^{-1}$  band is assigned to the  $[(\text{C}_5\text{H}_4)\text{Co}(\text{CO})(\text{PPh}_3)]^+$  side. The assignment of the  $2114$  and  $2091\text{ cm}^{-1}$  features to the  $[(\text{C}_5\text{H}_4)\text{Co}(\text{CO})_2]^+$  side is also supported by the fact that these bands are an average of about  $110\text{ cm}^{-1}$  higher than those of neutral  $\text{CpCo}(\text{CO})_2$  ( $2024$  and  $1958\text{ cm}^{-1}$ ), consistent with a one-electron change [17, 18]. The assignment of the  $2063\text{ cm}^{-1}$  band to the  $[(\text{C}_5\text{H}_4)\text{Co}(\text{CO})(\text{PPh}_3)]^+$  side is aided by measuring the actual spectrum of  $[\text{CpCo}(\text{CO})(\text{PPh}_3)]^+$ , obtained by chemical oxidation of an authentic sample of  $\text{CpCo}(\text{CO})\text{PPh}_3$  by  $[\text{Fc}][\text{B}(\text{C}_6\text{F}_5)_4]$  in  $\text{CH}_2\text{Cl}_2$  solution. In this experiment the  $1919\text{ cm}^{-1}$  band of the neutral compound was replaced by a new band at  $2063\text{ cm}^{-1}$  in the monocation,  $[\text{CpCo}(\text{CO})\text{PPh}_3]^+$  [19, 20].

Additional information about the structure of the substitution product is gained by considering the IR spectra of the neutral **2**. IR spectra recorded after back reduction of  $2^{2+}$  at a potential ( $E_{\text{appl}} = -0.7$  V) show the existence of another three IR bands shifted by  $100\text{ cm}^{-1}$  to lower energy at ( $2022$ ,  $1958$  and  $1925\text{ cm}^{-1}$ ) as shown in Fig. 5(c). The lower energy band,  $1925\text{ cm}^{-1}$ , can be directly assigned to the neutral monosubstituted side of **2** while the two bands at  $2022$  and  $1958\text{ cm}^{-1}$  comprise the neutral  $(\text{C}_5\text{H}_4)\text{Co}(\text{CO})_2$  side of **2** in addition to any regenerated neutral **1**. Of course, if the structure of  $2^{2+}$  was S1 (cis confirmation), there would still be three bands, but with little likelihood that they would match those of the two mononuclear analogues. From the IR data of  $2^{2+}$  and its neutral counterpart **2**, it can therefore be established that the substitution process occurs only at one side of the binuclear complex, **1**, giving a mono-substituted trans-derivative. On this basis, it is reasonable to assign the bands at  $2114$  and  $2091\text{ cm}^{-1}$  to the  $[(\text{C}_5\text{H}_4)\text{Co}(\text{CO})_2]^+$  side, a result that was inaccessible in the studies of the oxidation of  $\text{CpCo}(\text{CO})_2$  because of the rapid dimerization of the 17-electron cation  $[\text{CpCo}(\text{CO})_2]^+$  under these conditions [17, 18].

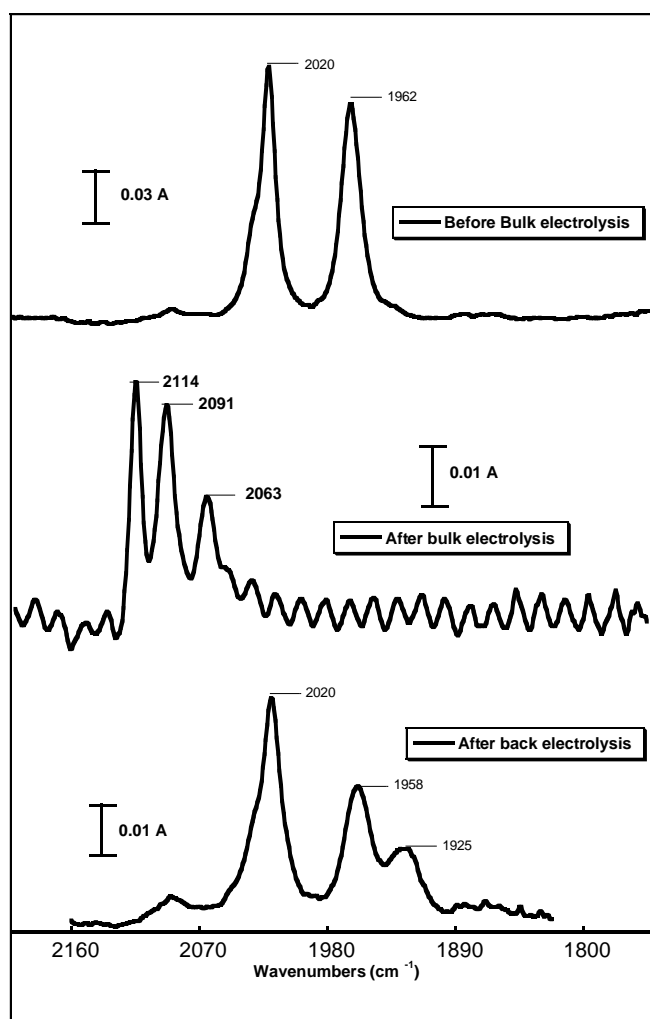
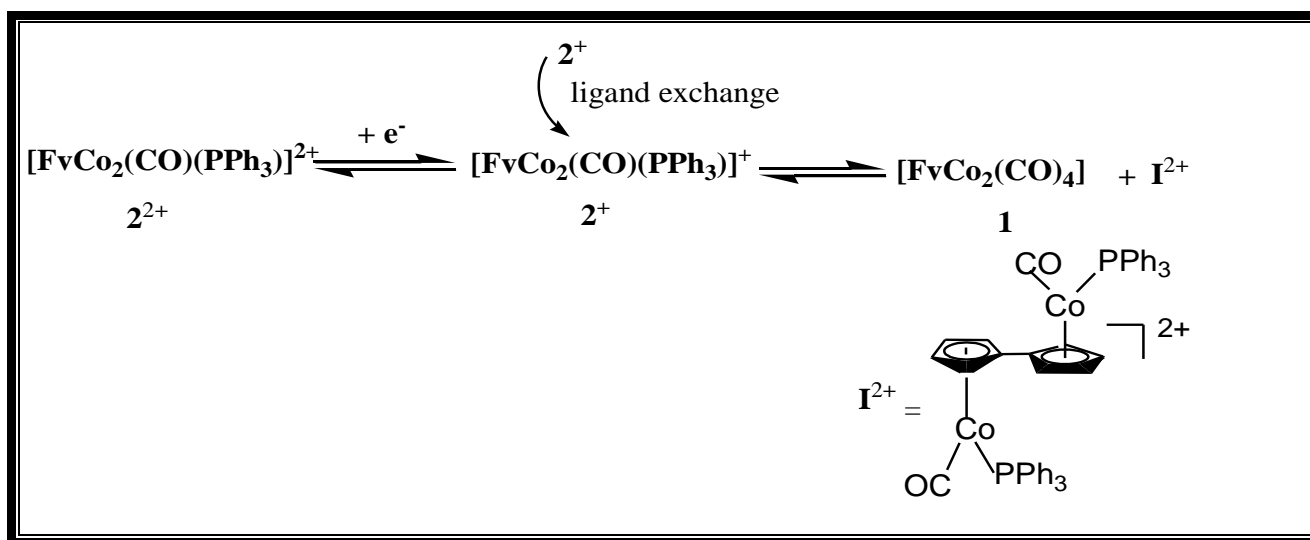


**Figure 5.** IR spectra of  $1\text{ mM } \mathbf{1}$  in  $\text{CH}_2\text{Cl}_2/0.05\text{ M } [\text{NBu}_4][\text{B}(\text{C}_6\text{F}_5)_4]$  and  $1\text{ equiv PPh}_3$  (a) Before bulk electrolysis. (b) After bulk electrolysis at  $E_{\text{app}} = 0.4\text{ V}$ . (c) After back electrolysis at  $E_{\text{app}} = -0.7\text{ V}$  vs  $\text{Fc}^{0/+}$  (Recorded using sampling technique).

To support these conclusions and get definitive information about the possible geometric structure of the substitution product **2**, we turned to ESR spectroscopy as another means to examine and identify the structure of the cation radical  $2^+$ . In order to record the ESR spectra of  $2^+$ , we first generated the  $\text{PPh}_3$ -monosubstituted dication,  $2^{2+}$  by bulk electrolysis as described above, after that the dication  $2^{2+}$  was electrochemically reduced to the monocation  $2^+$  by back electrolysis at  $E_{\text{app}} = -0.15$  V vs  $\text{Fc}^{0/+}$ . Ideally, at this applied potential the solution should contain only the mono-substituted monocation,  $2^+$ , but given the fact that the mononuclear analogue,  $[\text{CpCo}(\text{CO})\text{PPh}_3]^+$  is now known to undergo ligand exchange reaction [19], there is a possibility that similar reaction might occur upon the generation of the mono-substituted monocation  $[\text{FvCo}_2(\text{CO})_3\text{PPh}_3]^+$ ,  $2^+$ . Virtually, cyclic voltammograms recorded at 273 K after back electrolysis reveal the formation of  $2^+$  in addition to the regenerated neutral **1** (Fig. 6 (a)). The presence of the monocation  $2^+$  in the bulk solution was also confirmed via "steady-state" linear sweep voltammogram (Figure 6 (b)) obtained at scan rate of 2 mV/s, which clearly confirms the existence of  $2^+$  as evidenced by the cathodic current observed for wave **C** at  $E_{1/2} = 0.2$  V vs  $\text{Fc}^{0/+}$  and the anodic current for wave **D** at -0.35 V together with the two oxidation waves (**A** and **B**) of the parent **1**. The regeneration of neutral **1** upon back reduction of the mono-substituted dication,  $2^{2+}$ , can be explained based on the fact that  $2^+$  is probably undergoes CO-PPh<sub>3</sub> ligand-exchange reaction during its disproportionation to yield neutral **1** and the di-substituted dication as illustrated in Scheme 1. ESR of the fluid solution showed a single broad line ( $g$  value = 2.084 G) without coupling with either to the  $^{59}\text{Co}$  ( $I = 7/2$ ) or to the  $^{31}\text{P}$  ( $I = 1/2$ ) as shown in Fig. 7(a).



**Scheme 1.** The possible homogeneous and heterogeneous reaction pathways of  $2^+$

Similarly, the frozen solution ESR spectrum of  $2^+$  at 140 K (Figure 7(b)) shows very complicated hyperfine interactions with most likely a single  $^{59}\text{Co}$  ( $I = 7/2$ ) atom, although the exact nature of the splitting cannot be obtained from this spectrum. Other Co(II) systems such as  $[\text{Cp}^*\text{Co}(\text{CO})(\text{PPh}_3)]^+$  ( $\text{Cp}^* = \text{C}_5\text{Me}_5$ ) and  $[\text{CpCo}(\text{CO})(\text{PCy}_3)]^+$  ( $\text{Cy} = \text{cyclohexyl}$ ) have also been shown to exhibit similar hyperfine splitting pattern [23].

Significantly, qualitative comparison of the ESR spectra of  $2^+$  with that reported for  $[\text{FvCo}_2(\text{CO})_4]^+$ ,  $1^+$ , under similar conditions [16] shows that the fluid and the frozen spectra of the two cations are markedly different, thereby indicating that their structures are not similar. Since the monocation  $1^+$  was proved to have cis conformation with a partial formation of a Co-Co bond [16]. The likely structure for  $2^+$  is a trans-conformation, which is supported by the fact that the frozen ESR spectra of  $1^+$  and  $[\text{CpCo}(\text{CO})\text{PPh}_3]^+$  [16, 19] are qualitatively very similar. Apparently the large size and strong electron-donor  $\text{PPh}_3$  ligand induces the trans-configuration in  $2^+$  as a result of decreasing the positive charge around the Co atom, which facilitates the rotation of the Cp rings around the C-C bond.

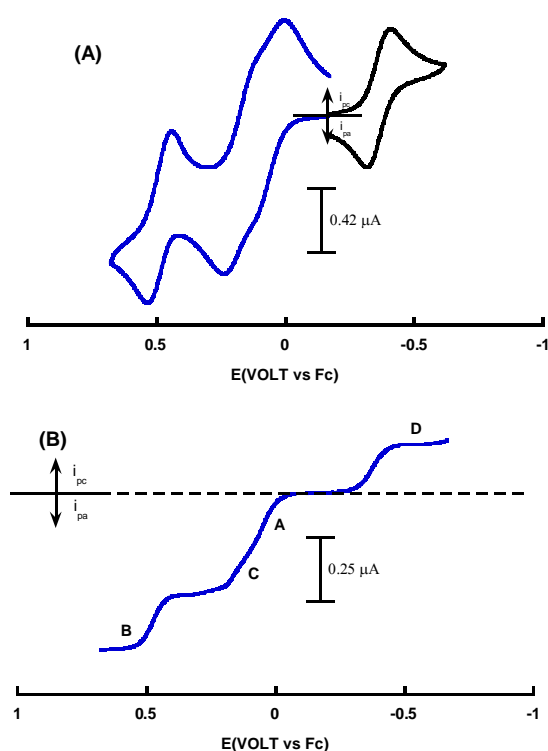


**Figure 6.** (a) Cyclic voltammograms recorded after back electrolysis of  $2^+$  at  $E_{\text{app}} = -0.15 \text{ V vs Fc}^{0/+}$  in  $\text{CH}_2\text{Cl}_2/0.05 \text{ M } [\text{NBu}_4][\text{B}(\text{C}_6\text{F}_5)_4]$  at scan rate of  $100 \text{ mV/s}$ ,  $1 \text{ mm}$  GC disk electrode. (b) LSV under the same conditions at scan rate of  $2 \text{ mV/s}$ .

IR spectra of the mono-substituted monocation,  $2^+$  exhibit three characteristic bands at  $2049$ ,  $2032$ ,  $1972 \text{ cm}^{-1}$ , respectively. The  $2049 \text{ cm}^{-1}$  band is assigned to the  $\{\text{Co}(\text{CO})(\text{PPh}_3)\}^+$  moiety, shifted slightly from the  $2063 \text{ cm}^{-1}$  of the dication  $2^{2+}$  owing to linkage with the neutral  $\text{Co}(\text{CO})_2$  group. Bands assigned to the  $\{\text{Co}(\text{CO})_2\}$  moiety in  $2^+$  (at  $2032$  and  $1976 \text{ cm}^{-1}$ ) are shifted by an amount that is similar in size, but opposite in direction, from neutral  $\text{Co}(\text{CO})_2$  groups in both **1** and **2**. In this case, the

shift to higher energy is rationalized by the linkage to the positively charged  $\{\text{Co}(\text{CO})(\text{PPh}_3)\}^+$  group. Since the spectral behavior is consistent with a model of charge localized at one center of the molecule with poor interaction with the other center, it is most likely that  $\mathbf{2}^+$  adopts the same structure as the dication  $\mathbf{2}^{2+}$ .

Owing to these voltammetric and spectroscopic results, it is clearly established that the oxidation of  $\mathbf{1}$  in presence of 1 equiv of  $\text{PPh}_3$  produces  $\text{PPh}_3$ -monosubstituted dication,  $\mathbf{2}^{2+}$ , as the ultimate oxidation product. Details of the mechanism associated with this electrochemically induced CO-substitution by  $\text{PPh}_3$  are illustrated in Scheme 2.

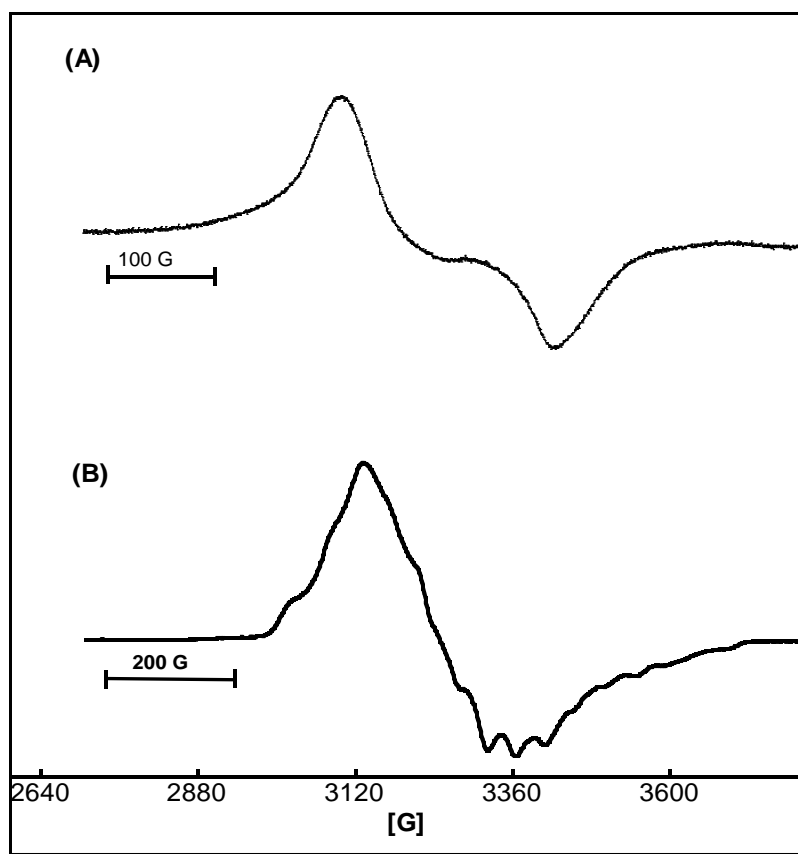
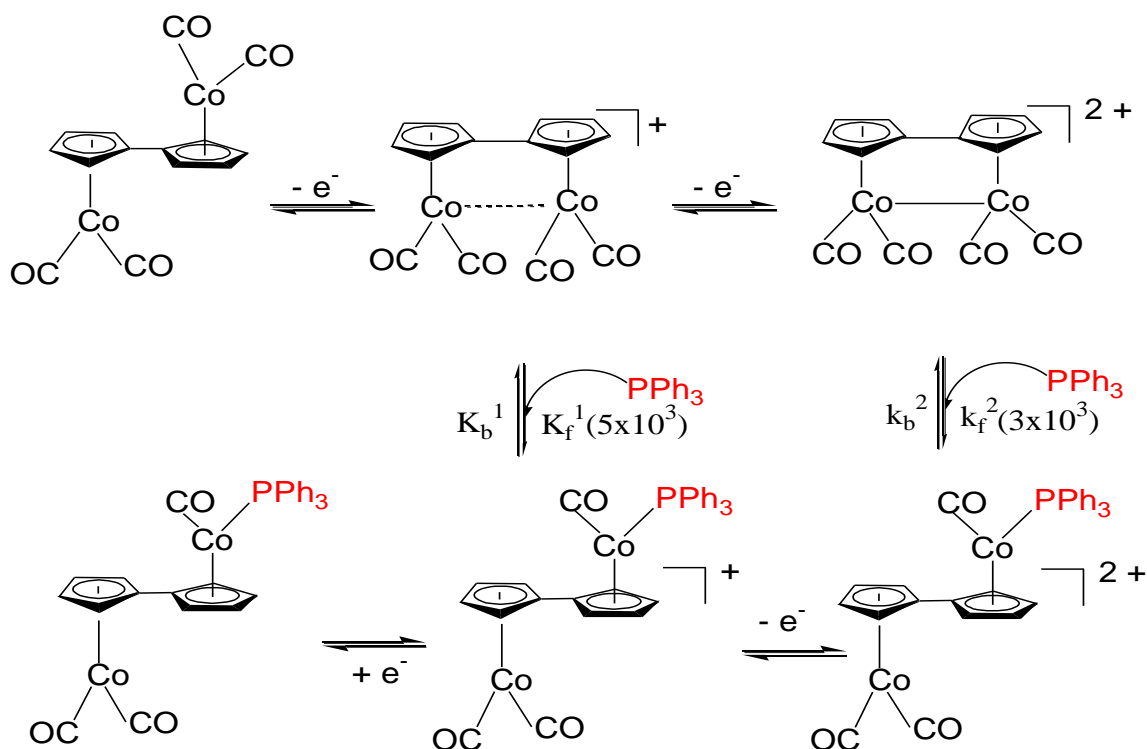


**Figure 7.** (a) Fluid solution ESR spectrum of the  $\mathbf{2}^+$  in  $\text{CH}_2\text{Cl}_2/0.05 \text{ M } [\text{NBu}_4][\text{B}(\text{C}_6\text{F}_5)_4]$ , 298 K and microwave power = 20 mW, modulation amplitude = 25.4 G. (b) ESR frozen spectrum of  $\mathbf{2}^+$  recorded at 140 K, microwave power = 40 mW, modulation amplitude = 5.069 G

Importantly, the negative potential for the  $\mathbf{2}^+/\mathbf{2}$  couple ( $E_{1/2} = -0.35 \text{ V}$ ) compared to  $\mathbf{1}/\mathbf{1}^+$  ( $E_{1/2} = 0.06 \text{ V}$ ) [16] testifies to the ease with which the neutral monosubstituted  $\mathbf{2}$  undergoes a one-electron oxidation. On this basis, the first oxidation wave of  $\mathbf{2}$  is shifted 410 mV negative from the comparable  $\mathbf{1}/\mathbf{1}^+$  couple. Since  $E_{1/2}$  is a measure of the electron richness of the neutral complex, the more negative potential is explained on the basis of the superior electron-donating ability of  $\text{PPh}_3$  compared to CO. Thus, the first oxidation of  $\mathbf{2}$  is attributed to the  $\text{PPh}_3$ -substitution side of the dinuclear complex.



**Scheme 2.** Showing the heterogeneous electron transfer and homogeneous CO-substitution reaction by  $\text{PPh}_3$

#### 4. SUMMARY AND CONCLUSIONS

Oxidatively-driven CO-substitution of  $\text{FvCo}_2(\text{CO})_4$ , **1**, by using  $\text{PPh}_3$  was accomplished using CV and bulk electrolysis procedures. In the presence of 1 equiv of  $\text{PPh}_3$  and on the CV time scale, the substitution reaction is straight forward, and yields the kinetically and thermodynamically stable mono-substituted product,  $[\text{FvCo}_2(\text{CO})_3\text{PPh}_3]^+$ , **2<sup>+</sup>**, that can be further oxidized at  $E_{1/2} = 0.2$  V to the corresponding mono-substituted dication,  $[\text{FvCo}_2(\text{CO})_3\text{PPh}_3]^{2+}$ , **2<sup>2+</sup>**, or reduced to neutral  $\text{FvCo}_2(\text{CO})_3\text{PPh}_3$ , **2** ( $E_{1/2} = -0.35$  V) complex. Formation of these substitution products over longer time scale via bulk electrolysis allowed for facile measurements of their spectroscopic properties using both IR and ESR spectroscopy. IR data revealed that the final product of the oxidative bulk electrolysis is the monosubstituted dication, **2<sup>2+</sup>**, evidenced by having three IR bands at 2114, 2091 and 2063  $\text{cm}^{-1}$ . This dication, **2<sup>2+</sup>**, can be easily reduced to the mono-substituted monocation, **2<sup>+</sup>**, or even the neutral **2** depending on the applied potential ( $E_{\text{app}}$ ) of the cathodic electrolysis. Back reduction of **2<sup>2+</sup>** at  $E_{\text{app}} = 0$  V generated the mono-substituted monocation, **2<sup>+</sup>**, which has also three IR bands, but at lower energies (2049, 2031, 1972  $\text{cm}^{-1}$ ). The fluid and frozen ESR spectra of **2<sup>+</sup>** are in a good agreement with its IR data and indicative of *transoid* geometry. The neutral mono-substituted, **2**, gave IR bands that are consistent with having one  $\text{Co}(\text{CO})(\text{PPh}_3)$  group (1925  $\text{cm}^{-1}$ ) and one  $\text{Co}(\text{CO})_2$  moiety (2022 and 1958  $\text{cm}^{-1}$ ). The latter has virtually the same IR frequencies as  $\text{CpCo}(\text{CO})_2$ .

The complexity of the substitution reaction of dinuclear complexes that contains two equivalent redox centers and more than one CO ligand compared to their mononuclear analogues stems from the fact that there is more than one possible pathway for the second phosphine to attack i.e., it is possible

for the second phosphine to attack either the first substituted center (leading to a di-substitution product on one side of the complex) or attack the second cobalt of the dinuclear complex (leading to two equivalent mono-substituted centers). To explore the possible mechanism(s) involved in this electrochemically promoted  $\text{PPh}_3\text{-CO}$  replacement reaction and to extract the thermodynamic and kinetic parameters of the underlying homogeneous and heterogeneous reactions, one should perform digital simulation of the generated cyclic voltammetric data under these conditions. This study will be addressed in details in a following paper. Significantly, the performance of this electrochemically-induced CO-substitution reaction of the dinuclear  $\text{FvCo}_2(\text{CO})_4$  is made possible by the greatly enhanced stability of its generated radicals in media comprising gentle solvent/electrolyte media.

#### ACKNOWLEDGMENT

The authors would like to extend their sincere appreciation to Scientific Research at King Saud University for funding through the Research Group Project no RGP-VPP-236.

#### References

1. G.L. Geoffroy, M.S. Wrighton, "*Organometallic photochemistry*", Academic Press: New York, 1979.
2. K. Koike, N. Okoshi, H. Hori, K. Takeuchi, O. Ishitani, H. Tsubaki, I.P. Clark, M. W. George, F.P.A. Johnson, J.J. Turner, *J. Am. Chem. Soc.*, 124 (2002) 11448.
3. J.A. van Rijn, E. Gouré, M.A. Siegler, A.L. Spek, E. Drent, E. Bouwman, *J. Organomet. Chem.* 696 (2011) 1899
4. J.L. Clark, S.B. Duckett, *J. Chem. Soc., Dalton Trans.*, 43 (2014) 1162.
5. K.R. Mann, G.S. Hammond, H.B. Gray, *J. Am. Chem. Soc.* 99 (1977) 306.
6. M.C. Baird, *J. Organomet. Chem.* 50 (2014) 751
7. R.A. Rossi, A.B. Pierini, A.B. Penénory, *Chem. Rev.*, 103 (2003) 71.
8. W.E. Geiger, *Organometallics* 26 (2007) 5738.
9. A. Houmam *Chem. Rev.*, 108 (2008) 2180.
10. J.W. Hersberger, R.J. Klingler, J.K. Kochi, *J. Am. Chem. Soc.*, 105 (1983) 61.
11. D.A. Sweigart, "*Mechanisms of Inorganic and Organometallic Reactions*", Twigg, M.V., Ed.; Plenum: New York, 1985; Chapter 10, pp 263-281
12. H.-J. Langenbach, H. Vahrenkamp, *Chem. Ber.* 110 (1977) 1195.
13. H.-J. Langenbach, H. Vahrenkamp, *Chem. Ber.* 112 (1977) 3391.
14. R.T. Baker, J.C. Calabrese, P.J. Krusic, M.J. Therien, W.C. Trogler, *J. Am. Chem. Soc.*, 110 (1988) 8392.
15. M.I. Bruce, D.C. Kehoe, J.G. Matison, B.K. Nicholson, P.H. Rieger, M.L. Williams, *J. Chem. Soc., Chem. Commun.* (1982) 442.
16. A. Nafady, W.E. Geiger, *Organometallics* 27 (2008) 5624.
17. N. Camire, A. Nafady, W. E. Geiger, *J. Am. Chem. Soc.* 124 (2002) 7260.
18. A. Nafady, P. J. Costa, M. J. Calhorda, W. E. Geiger, *J. Am. Chem. Soc.* 128 (2006) 16587.
19. A. Nafady, W. E. Geiger, *Organometallics* 29 (2010) 4276.
20. A. Nafady, R. A. Ammar, H. M. El Sagher, U. A. Rana, K. A. AL-Farhan *Int. J. Electrochem. Sci.* 8 (2013) 1700.
21. R.J. LeSuer, W.E. Geiger, *Angew. Chem., Int. Ed.* 39 (2000) 248.
22. W.E. Geiger, "*In Laboratory Techniques in Electroanalytical Chemistry*", 2<sup>nd</sup> ed.; P.T. Kissinger, W.R. Heineman, Eds.; Marcel Dekker: New York, (1996); Chapter 23.

23. K. Broadley, N.G. Connelly, W.E. Geiger, *J. Chem. Soc., Dalton Trans.* (1983) 121.
24. W.E. Geiger, *Coord. Chem. Rev.* 257 (2013) 1459.

© 2015 The Authors. Published by ESG ([www.electrochemsci.org](http://www.electrochemsci.org)). This article is an open access article distributed under the terms and conditions of the Creative Commons Attribution license (<http://creativecommons.org/licenses/by/4.0/>).